Primljen / Received: 29.5.2020.
Ispravljen / Corrected: 3.9.2020.
Prihvaćen / Accepted: 10.9.2020.
Dostupno online / Available online: 10.11.2020.

Strengthening of masonry walls with FRP or TRM

Authors:

[1]Prof. Tomislav Kišiček, PhD. CE
tomislav.kisicek@grad.unizg.hr

[1]Assist.Prof. Mislav Stepinac, PhD. CE
mislav.stepinac@grad.unizg.hr

[1]Tvrtko Renić, MCE
tvrtko.renic@grad.unizg.hr
Corresponding author

[1]Ivan Hafner, MCE
ivan.hafner@grad.unizg.hr

[1]Luka Lulić, MCE
luka.lulic@grad.unizg.hr

[1] University of Zagreb
Faculty of Civil Engineering

Subject review

Tomislav Kišiček, Mislav Stepinac, Tvrtko Renić, Ivan Hafner, Luka Lulić

Strengthening of masonry walls with FRP or TRM

In addition to traditional methods of strengthening shear masonry walls, some newer materials and systems, such as fibre reinforced polymers (FRP) and textile reinforced mortars (TRM), have recently been introduced. The earthquake that occurred in Zagreb and its surroundings on 22 March 2020 has revealed the sensitivity of unreinforced masonry buildings to horizontal actions, while pointing to the need to repair damage to load-bearing and non-load-bearing walls and to strengthen walls against shear failure. Existing regulations do not cover design of structures with such systems. The paper presents modern procedures for strengthening masonry with FRP or TRM, scientific research in this area, advantages and disadvantages, and calculation of such reinforcements.

Key words:
earthquake, walls, shear, FRP, TRM, existing structures, analysis

Pregledni rad

Tomislav Kišiček, Mislav Stepinac, Tvrtko Renić, Ivan Hafner, Luka Lulić

Pojačanje zida na posmik pomoću FRP-a ili TRM-a

U novije vrijeme uz tradicionalne metode pojačanja zida na posmik, koriste se i noviji materijali i sustavi kao što su polimeri armirani vlaknima (FRP) i tekstilom armirani mortovi (TRM). Potres koji se dogodio u Zagrebu i okolici 22. ožujka 2020. pokazao je osjetljivost nearmiranih zidanih zgrada na horizontalna djelovanja, potrebu za sanacijom oštećenja na nosivom i nenosivom zidu i pojačanjem zida na posmik. Postojeći propisi ne pokrivaju proračune pojačanja s takvim sustavima. U radu su prikazani suvremeni postupci pojačanja zida FRP-om ili TRM-om, znanstvena istraživanja iz tog područja, prednosti i nedostaci te proračun takvih pojačanja.

Ključne riječi:
potres, zide, posmik, FRP, TRM, postojeće konstrukcije, proračun

Übersichtsarbeit

Tomislav Kišiček, Mislav Stepinac, Tvrtko Renić, Ivan Hafner, Luka Lulić

Schubbewehrung von Wänden mit FRP oder TRM

In jüngerer Zeit werden neben herkömmlichen Verfahren zur Schubbewehrung von Mauerwerk auch neuere Materialien und Systeme wie faserverstärkte Polymere (FRP) und textilverstärkter Mörtel (TRM) verwendet. Das Erdbeben in Zagreb und Umgebung am 22. März 2020 zeigte die Empfindlichkeit von nicht bewehrten Mauerwerksgebäuden gegenüber horizontalen Einwirkungen, die Notwendigkeit, Schäden am tragenden und nicht tragenden Mauerwerk zu reparieren und die Wände gegen Abscheren zu bewehren. Bestehende Vorschriften gelten nicht für Bewehrungsberechnungen mit solchen Systemen. Die Arbeit präsentiert moderne Verfahren zur Bewehrung von Mauerwerk mit FRP oder TRM, wissenschaftliche Forschungen auf diesem Gebiet, Vor- und Nachteile sowie die Berechnung solcher Bewehrungen.

Schlüsselwörter:
Erdbeben, Mauerwerk, Scherung, FRP, TRM, bestehende Strukturen, Berechnung

1. Introduction

Earthquakes are a natural phenomenon that cannot be predicted. Although it is possible to predict where an earthquake of a certain magnitude might occur, it can not be envisaged when such an event could happen. It is known that Zagreb and the entire Croatia lies in a seismically active area. It is also known that Zagreb and its surroundings were hit by stronger earthquakes in the past and that the last one, of magnitude 6.3 according to the Richter scale, occurred in 1880 [1, 2].

It had always been clear that a similar earthquake would come, but it was not known when it could happen. Unfortunately, on 22 March 2020, Zagreb and its surroundings were hit by an earthquake of magnitude 5.5 according to the Richter scale, which was followed by another 5.0 magnitude earthquake, and several smaller ones that occurred in the days after the main earthquake. The epicentre was 7 km from the centre of Zagreb, around Markuševec. The old town (Upper Town and Lower Town) and suburban areas of Čučerje and Markuševec suffered the greatest damage.

The buildings in the city centre are typical masonry structures built in the late 19th and early 20th century. They are made of solid brick, masonry is unreinforced, floor structures are wooden beams, and the roof is a wooden structure covered with tiles. Due to their age, i.e. exceedance of planned service life, construction prior to adoption of seismic regulations, and poor or inadequate maintenance, such buildings suffered the greatest damage in this earthquake. Even some newer buildings that were designed for significantly lower seismic load compared to that required by modern regulations, also suffered extensive damage [3].

Regulations for the construction of facilities in seismically active areas have been developed over the past fifty years. The introduction and development of regulations was prompted by earthquakes that occurred in the nearby areas (Skopje, Banja Luka, Dubrovnik and Montenegro, Ston) [4]. Therefore, the extent of damage to buildings is reduced if modern construction systems, increasingly advanced design regulations, innovative materials and structural systems, are used [5].

Old masonry structures, in addition to their considerable weight, rigidity and low ductility, are also characterized by poor quality of materials and inadequate construction, which is due to lack of regulations and control at the time they were built [6]. Therefore, behaviour of masonry structures during earthquakes is hampered by significant limitations [7]. Newer masonry structures that are reinforced or confined by reinforced concrete elements possess a certain level of seismic resistance and ductility. The most vulnerable are the oldest unreinforced masonry structures that have low or almost nil level of seismic resistance. Many of such buildings belong to cultural heritage, which is an additional motive for their preservation [8]. In addition, poor maintenance by the owners, as well as many unfavourable interventions and renovations, have further diminished the safety of such buildings.

During an earthquake, unreinforced masonry walls can fail either in their plane and/or out of their plane. There are three in plane failure mechanisms: bending failure, shear sliding failure along horizontal joint, and diagonal shear failure (straight or stepped), the last one being also the most recognizable due to its frequent occurrence in areas affected by earthquakes [9]. Figure 1 shows characteristic damage to masonry walls caused by the Zagreb earthquake of 22 March 2020.

Many failure modes are possible outside of the plane because of poor interconnection of perpendicular walls and poor wall-floor connections. All these failures were, unfortunately, registered after the recent earthquake in Zagreb, which points to the sensitivity of unreinforced masonry structures to horizontal actions.

Initial assessment of earthquake-damaged buildings is followed by a long-term process of renovation and strengthening. Renovation alone is not sufficient because it would bring the damaged structure to a pre-earthquake condition characterized by inadequate seismic resistance. Therefore, it is extremely important to increase seismic resistance of existing buildings so as to improve their behaviour during future seismic events. In addition to traditional strengthening methods, such as reinforced concrete jacketing or grouting, the use will certainly be made of more recent materials that present numerous advantages. Newer materials include fibre-reinforced polymers (FRP). Over the years, numerous studies have been conducted with regard to the use of FRP for strengthening numerous types of structures made of various materials. Main advantages of FRP lie in low self-weight and high strength. Despite many advantages of FRP, this material also presents certain disadvantages. These disadvantages have encouraged development of innovative high-quality textile reinforced mortars (TRM). Modern procedures for strengthening unreinforced masonry walls with FRP and TRM are described and compared in the following sections, where suitable calculations and results of latest scientific research in this field are also presented.

Figure 1. Masonry damage caused by Zagreb earthquake of 22 March 2020

2. New materials for strengthening masonry structures: FRP and TRM

2.1. FRP

FRP or fibre reinforced polymer is a fibrous composite material in which fibres, assuming the function of reinforcement, are embedded in a polymer matrix that provides the final shape [10]. The first FRP was developed in 1909 while the

mass production in various branches of industry began in the 1970s. The type and orientation of fibres, the composition and quantity of the matrix, and the method of production, significantly influence the characteristics of the final product. The production process involves production of textiles (weaving, knitting, or sewing) which are then joined with the polymer matrix manually, semi-automatically, or automatically [11]. Carbon fibre textile, and glass and carbon fibre textile, are shown, from left to right, in Figure 2. The most common method of production is pultrusion (fully automated), an extrusion-like process used in the production of aluminium and mild steel profiles [12].

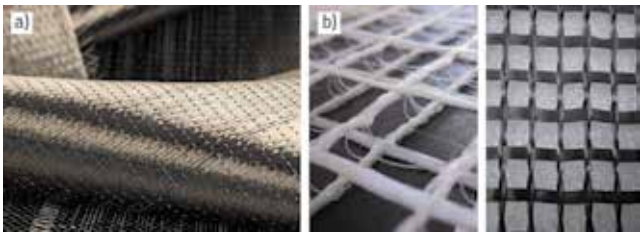

Figure 2. a) Carbon fibre textile [13], b) glass and carbon fibre textile [14]

Main advantages of FRP are corrosion resistance, light weight (approximately ¼ of the weight of steel), and high tensile strength. Excellent corrosion resistance is mostly used in reinforced concrete structures in aggressive environments by using FRP reinforcement [15], and also as a means to strengthen exposed structural elements [16]. Light weight makes it easier to apply FRP in confined spaces and eliminates the need for formwork, which reduces labour costs. Other favourable characteristics are a significant strength to weight ratio, good behaviour under dynamic load, insensitivity to magnetism, non-conduction of electric current, ability to dampen vibrations, resistance to most acids and alkalis, ability to assume various shapes and lengths, ease and speed of application [17, 18]. Disadvantages include linear-elastic behaviour to failure, i.e. non-ductility, in contrast to steel, which exhibits elastoplastic behaviour, i.e. ductility. In addition, the cost of material is relatively high, and epoxy-resin properties degrade at temperatures higher than the glass transition temperature (e.g. in the case of fire) [19]. FRP reduces the vapour permeability of the structure and makes it difficult to assess damage after an earthquake. FRP can not be applied in the case of incompatible or wet surfaces and low temperatures. There are several types of fibres and, hence, FRP products: glass fibres (GFRP), carbon fibres (CFRP), aramid fibres (AFRP) and basalt fibres (BFRP), while epoxy, unsaturated polyester, vinyl ester, bismaleimide, and cyanate ester resins are used to make matrices. Also, the following FRP-based strengthening systems can be distinguished: wet lay-up, prefabricated systems and special systems (automated wrapping, prestressed FRP strips, and inserted FRP strips) [20]. Figure 3 graphically shows the areas in which stress-strain diagrams of individual types of FRP are located, and provides their comparison with the stress-strain diagram of mild steel.

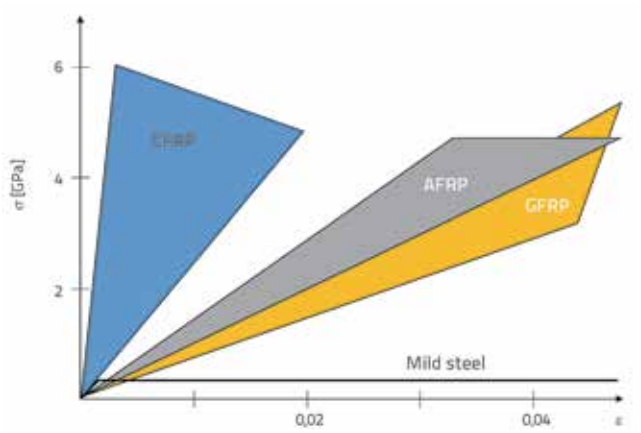

Figure 3. Uniaxial tension stress–strain diagrams for FRPs and steel [19]

2.1.1. Fibres

Glass fibres have lower strength (1800 – 3600 MPa), lower modulus of elasticity (70 – 76 GPa) and higher weight (2270 – 2600 kg/m^3) compared to carbon fibres, but they are cheaper and therefore the most widely used. They are produced at high temperatures from a mixture of molten rock sand, kaolin, limestone, and colemanite. Glass varieties are: alkaline A-glass, electric E-glass, and chemical C-glass. The biggest drawback of glass is its sensitivity to alkaline corrosion, which emphasizes the importance of protective role of polymer matrix (in FRP) as it prevents penetration of alkali to the fibres.

Carbon fibres have high strength (2500 – 4000 MPa) and high modulus of elasticity (200 – 650 GPa). They are resistant to corrosion as well as to creep and fatigue, but their impact strength is low. They are produced from PolyAcryloNitrile (PAN), tar, bitumen, and cellulose, by controlled oxidation, carbonization, and graphitization of organic substances. Depending on the graphitization temperature, carbon fibres can be either high-strength fibres (2600 °C) or fibres with high modulus of elasticity (3000 °C).

Aramid fibres are synthesized polymers which, in addition to high strength (3500 – 4200 MPa), also exhibit resistance to impact load, thermal influences, and deterioration due to chemical influences, but are less resistant to UV radiation. Commercial names of aramid fibres are Kevlar, Twaron, Technora and SVM [20].

Basalt fibres have been used over the last 10 years now to strengthen masonry. They have significantly lower tensile strength (1100 MPa) compared to carbon fibres, which is further reduced, as well as the volume stability, in an alkaline environment. In order to reduce alkaline effects of the matrix (mortar in TRM) on the fibres, they are factory coated with a protective coating. They exhibit significantly higher thermal stability and heat resistance compared to carbon and glass fibres [21].

2.1.2. Matrices

Polymer matrices are as important as fibres. They connect the fibres and provide them with protection from external influences. The shear strength of the bond between the fibres and the matrix that transmits loads to the fibres is crucial for mechanical properties of the composite.

Epoxy resins are suitable for various production methods, and so desired mechanical properties can easily be adjusted in advance depending on the requirements.

Unsaturated polyester and vinyl ester resins are extremely sensitive to the presence of water due to solubility of esters, which leads to a significant decrease in shear resistance between composite layers. These resins also exhibit significant shrinkage (8 %) during transition from liquid and semi-solid state to solid state, which causes internal stresses that further reduce the strength of the composite.

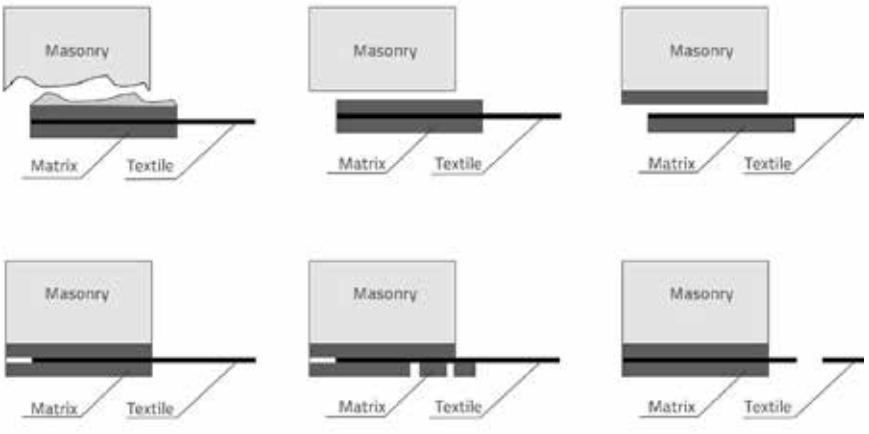

Figure 4. Failure modes [25]

Bismaleimide resins are expensive but have excellent chemical resistance and dimensional stability. They retain good mechanical properties even at high temperatures (up to 120 °C).

Cyanate ester resins are also pricey and they exhibit excellent mechanical properties that they retain even at high temperatures (up to 175 °C) [20].

2.1.3. Strengthening systems

In order to achieve a quality connection between the FRP and wall surface, the conditions at the installation site and the quality treatment of the wall surface are extremely important. Care must also be taken to ensure the quality and full compatibility of all components in order to avoid separation of the FRP from the substrate.

Wet lay-up system is most commonly used because of its simplicity, economy, and versatility. In order to achieve a good connection between the masonry and the FRP, a base coat is applied to the surface of the masonry before the adhesive.

Prefabricated FRP systems most often appear in the form of a strip and are used mainly to strengthen elements subjected to bending load.

Special FRP systems are used in situations where standard FRP strengthening systems are not possible or not economical. Such systems are, for example, automated wrapping systems mainly used for columns, systems with inserted FRP strips and systems with prestressed FRP strips where the FRP strips are prestressed before gluing and anchoring, thus improving the strengthening effect [20].

2.2. TRM

TRM or textile reinforced mortar is a more recent composite formed by replacing an organic binder (matrix) with an inorganic one (cement or lime mortar) in order to solve the stated shortcomings of FRP [22]. The terms FRCM (fabric-reinforced cementitious matrix), MBC (mineral-based composite) and TRC (textile-reinforced concrete) are also used in the literature for TRM [23]. These materials consist of textiles made of fibre bundles (glass (G), carbon (C), basalt (B) or Polyphenylene benzobisoxazole (PBO) fibres) in at least two (usually orthogonal) directions and an inorganic matrix, and so GTRM, CTRM, BTRM, or PBOTRM can be differentiated. The fibres take on tensile stresses, while the matrix protects the fibres and transmits stresses from the wall that is being strengthened to the fibres. The density of the mesh, i.e. the amount of fibre bundles and their spacing, can be controlled independently in each direction, which affects the mechanical properties of the textile and the degree of penetration into the mortar through the mesh. Adhesion between the textile and mortar is achieved by mechanical wedging, which is a result of mortar penetrating between fibres that make up the mesh. TRM increases the resistance of masonry to shear and bending in the plane, bending out of the plane, while also increasing vertical load-bearing capacity. It is also used to strengthen masonry arches, vaults and domes [24]. The problem that appears during shear strengthening of masonry walls is the connection between the applied strengthening and the masonry. A quality connection between the substrate and the matrix, and between the matrix and the textile, is required to achieve the transfer of forces from the wall to the TRM, and to obtain a composite effect. It can be improved by mechanically anchoring TRM layers to the wall. Figure 4 shows shear failure modes of the connection between the TRM and masonry.

TRM composites are placed in the same way as FRP composites, most often by the "hand lay-up" method. First a layer of mortar is applied, then a layer of mesh, and then again a layer of mortar, and the procedure is repeated depending on the desired number of layers. It is important that each layer of mortar is applied while the previous one is still fresh (Figure 5).

Figure 5. TRM application [26]

The behaviour of tensile loaded TRM in the idealized bilinear diagram proposed by AC434 ICC-ES [27] is shown in Figure 6 where f_{fu} is the maximum tensile stress of the TRM and ε_{fu} is the corresponding maximum tensile strain. f_{ft} represents the tensile stress at which the TRM cracks and ε_{ft} the corresponding tensile strain. The general stress and the corresponding tensile strain are marked as f_{fi} and ε_{fi}, respectively. The modulus of elasticity before cracking is denoted by E_f^* and the modulus of elasticity after cracking by E_f.

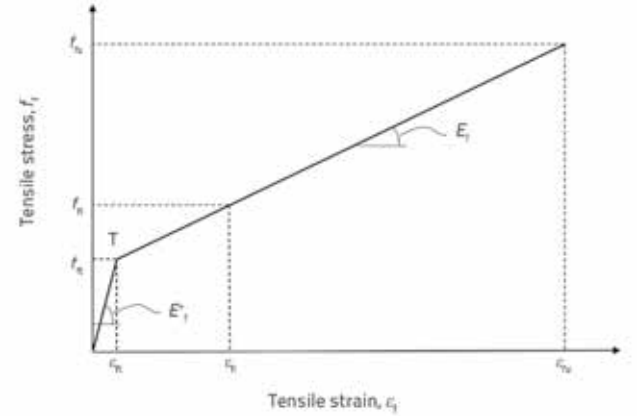

Figure 6. Tensile stress-strain diagram for TRM

Mechanical properties of TRM are well known while its durability with respect to exposure to external influences has so far been insufficiently investigated [28].

2.3. Comparison of FRP and TRM

Both systems significantly contribute to the ductility, load-bearing capacity and, to a lesser extent, to wall rigidity outside the plane and in the plane, but there are also certain differences. FRP has been used longer and is more favourable for concrete, but TRM has been developed due to the need to improve some of the FRP shortcomings. By using an inorganic matrix instead of resin, TRM is more favourable for structural strengthening and renovation of masonry structures [22]. Unlike FRP, the inorganic matrix of TRM allows installation even in unfavourable conditions such as cold and damp masonry surfaces [29]. The lack of vapour permeability in FRP can lead to structural damage. FRP and TRM also differ in behaviour under the influence of high temperatures where TRM's inorganic matrix shows better properties than FRP's epoxy matrix, which experiences degradation of properties. In addition to being non-flammable and non-toxic when exposed to fire, TRM also contributes to fire resistance of the wall itself due to an additional protective layer. Ignition of FRP or release of additional heat was not observed during testing, but pyrolysis and matrix decay were observed [30]. With FRP and TRM, it is possible to strengthen the walls on one or both sides and, in the latter case, they will significantly increase the load-bearing capacity, while also ensuring symmetry of the wall stiffness. On the other hand, one-sided strengthening leads to different stiffness on the strengthened and non-strengthened sides of the wall. Such a difference in stiffness leads to out of plane bending and, possibly, to out of plane failure [31]. Both methods of strengthening contribute greatly to the bending and shear resistance of masonry. However, premature separation of FRP or TRM strips or meshes from the surface of the masonry is a limitation of these techniques. In order to solve or mitigate the problem of separation, it is necessary to ensure proper anchoring of FRP or TRM [32]. According to ICOMOS (International Council of Monuments and Sites) guidelines, it is more acceptable to use TRM because it complies with a number of building conservation requirements.

3. Behaviour of masonry under shear

A masonry loaded with horizontal forces in a plane is subject to shear. Failure occurs if shear capacity is exceeded. Three basic modes of wall failure when loaded in plane are: diagonal failure, bending failure, and sliding failure. These failure modes are shown in Figure 7.

Failure modes a) and c) can be considered as shear failure modes. Which failure mode will occur depends on wall geometry and wall material used, but also on the amount of vertical load. When a very small amount of vertical load is applied, sliding can occur along one horizontal joint. Bending moment and shear occur as a result of lateral force. When a wall is subjected to small vertical force, a horizontal crack opens at a small bending moment, and this crack spreads through a significant part of the cross section; due to a small or non-existent compression area, the shear force causes the wall to "slide" on one joint or overturn. This joint may or may not be at the bottom of the element. Inadequate realisation, poor mortar quality, or change of material, can cause a weak surface in the wall. Although the existing horizontal crack is partially or completely closed in each cycle, the material has lost cohesion due to cracking, and this crack is in effect a "trace line" along which failure is most likely to occur. In the earthquake of 22 March 2020, this failure mode was characteristic

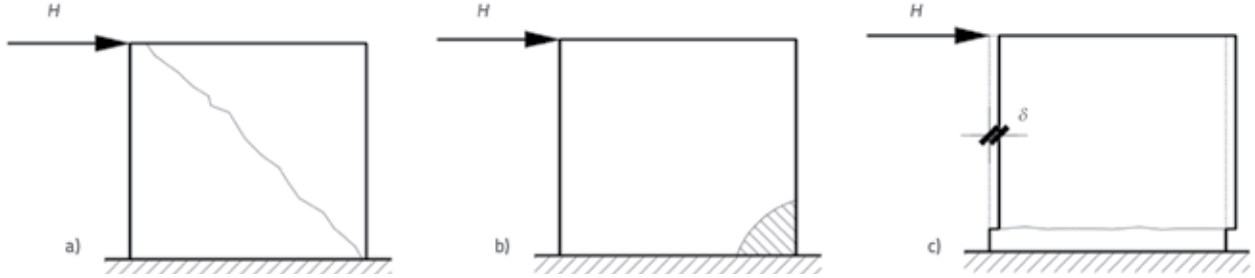

Figure 7. Failure modes: a) diagonal failure, b) bending failure, c) sliding failure

for chimneys that mostly failed along one horizontal joint. Sliding failure can be described by the Mohr-Coulomb model of material behaviour, i.e.:

$$f_v = f_{v0} + \mu \cdot \sigma_d \quad (1)$$

where:
f_v - shear strength of masonry
f_{v0} - initial shear strength of masonry (component independent of vertical force)
μ - coefficient of friction (tanϕ), where ϕ is the angle of internal friction
σ_d - design vertical compressive stress.

For existing masonry, it is recommended to use mean values of material characteristics, while characteristic values are used for the new masonry. For existing walls, that means **μ** = 0,5, and f_{v0} = 0,1 MPa is to be used according to recommendations given in [33]. For new masonry **μ** = 0,4. According to newly proposed EN 1998-3 [34], the recommendation is f_{v0} = 0,16 MPa.
It is assumed in this model that the shear is transferred only by the compressive part of the cross section because friction is not activated in tension (the assumption is that there is no material contact), and cohesion is considered non-existent in tension because the element is cracked. The partial safety factor according to the current EC 1998-3 [34] is the product of the partial factor for the material, i.e. two thirds of the value of γ_M according to [35] and the confidence factor. According to the new proposal of EC 1998-3 [34], the material is not corrected, but rather the load-bearing capacity, i.e. a partial safety factor is used for resistance γ_{Rd} (confidence factor and γ_M are not used) whose value depends on the level of knowledge and type of failure. The partial safety factor γ_{Rd} for sliding failure is 1,65 for the lowest level of knowledge, 1,5 for the intermediate level and 1,35 for the highest level of knowledge. Shear capacity can be determined by Eq. (2)::

$$V_{p,Rd} = \frac{1}{\gamma_{Rd}} \cdot f_v \cdot L_c \cdot t_w \quad (2)$$

where:
γ_{Rd} - partial safety factor for resistance
L_c - length of masonry in compression
t_w - wall thickness.

Diagonal failure is characteristic for moderate amount of vertical compressive force, which is a very common case in the lower parts of the structure. The crack can pass through the brick and mortar, or only through the mortar (stepped failure mode). Stepped failure mode is a combination of tension perpendicular to the head joint (tensile strength of the contact between the mortar and the wall element) and slipping on a series of horizontal surfaces. The crack spreads through the brick mainly in case the brick is of poor quality and the mortar is of good quality, while a stepped failure is characteristic otherwise. Also, "straight" diagonal failure is common when wall elements are irregular. Diagonal failure modes are more common in older masonry, so the currently valid standard HRN EN 1996-1-1 [35] does not consider this failure mode. The standard EN 1998-3 [34] also does not consider this failure mode. These failure modes are considered as being mostly relevant for existing masonry in proposals of the next generation of this standard. A stepped failure is shown in Figure 8.a, and a "straight" diagonal tensile failure is shown in Figure 8.b.

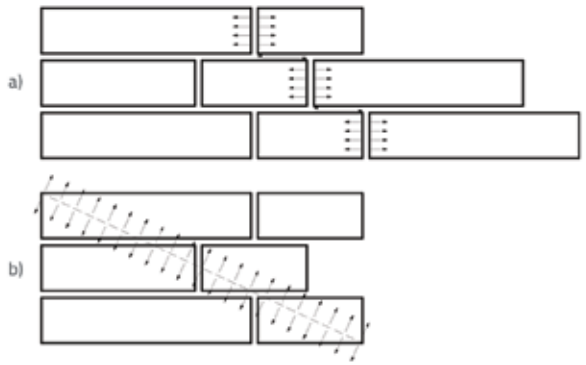

Figure 8. Diagonal tension failure modes: a) stepped b) "straight"

Straight diagonal failure occurs due to exceedance of main inclined tensile stresses. In accordance with the theory of elasticity according to the paper by Turnšek i Čačovič [36] the tensile strength is:

$$f_t = -\frac{\sigma_0}{2} + \sqrt{\left(\frac{\sigma_0}{2}\right)^2 + (b \cdot \tau)^2} \quad (3)$$

where:
σ_0 - average vertical compressive stress (over the entire surface of the wall)
b - geometry factor ($b = h/L$, but between 1 and 1.5)
h - wall height
L - wall length (total)
τ - shear stress.

The geometry factor b is the shear stress distribution factor which depends on the height to length ratio of the wall. Eq. (3) can be written by expressing the allowable shear stress based on the known tensile strength and vertical pressure, Eq. (4):

$$\tau = \frac{f_t}{b} \cdot \sqrt{1 + \frac{\sigma_0}{f_t}} \quad (4)$$

Shear capacity can be determined by Eq. (5):

$$V_{t1,Rd} = \frac{1}{\gamma_{Rd}} \cdot L \cdot t_w \cdot \frac{f_t}{b} \cdot \sqrt{1 + \frac{\sigma_0}{f_t}} \quad (5)$$

The partial safety factor γ_{Rd} for regular masonry in both modes of diagonal failure is 1.7 for the lowest level of knowledge, 1.55 for the intermediate level of knowledge, and 1.4 for the highest level of knowledge. These two failure modes were considered in [37] and the test results showed that diagonal failure (both

straight and stepped) can be more appropriately described by Eq. (5). Although it seems logical that a stepped failure could be described by Eq. similar to the one for slidin failure (this procedure is described later), especially if tensile strength is neglected, the multi-level failure still remains as a problem. If the case from Figure 9 is considered, it is clear that different sections along the height of the wall have different lengths of the compression area. Bending moment at the top is zero (for the cantilever) and is significantly higher at the bottom, while the compressive force is approximately constant. The whole element is usually in compression in the cross-sections at the top, while a significant part of the cross-section can be in tension in the cross-sections at the bottom. The question is what length of compression area should be used in Eq. (2) to describe stepped failure. It is obvious that the length at the bottom will often give an excessively small load-bearing capacity, and the problem is complicated by the fact that boundary conditions of real walls are more complex than the case shown in Figure 9.

According to [7], the value of f_{tk} = 0.09 MPa can be assumed for old masonry if there are no test results, which means that the mean value of tensile strength is 0.11 MPa (for existing masonry). According to the new proposal of EN 1998-3 [34], the mean value of tensile strength for solid brick walls with lime mortar is 0.114 MPa.

The stepped failure mode can be most accurately described by an Eq. similar to that used for slidin, albeit with some modifications. An Eq. describing a stepped failure mode is given in [38] (later modified in [39, 40]). An overview of various failure modes, with standards in which these modes are described, is given in [41]. It is important to note that the stepped failure mode is described in a number of standards by Eq. (6). One of such methods is in the future version of EN 1998-3 [34], which is intended for seismic design of existing structures. Shear capacity at stepped failure can be determined by the Eq. (6):

$$V_{t2,Rd} = \frac{1}{\gamma_{Rd}} \cdot \frac{L \cdot t_w}{b} \cdot \left(\frac{f_{v0}}{1+\mu_j \cdot \phi} + \frac{\mu_j}{1+\mu_j \cdot \phi} \cdot \sigma_0 \right) \leq V_{d,lim} \qquad (6)$$

where:

μ_j - local coefficient of friction of the joint, if more accurate data are not available, amounts to 0.6

ϕ - clamping coefficient.

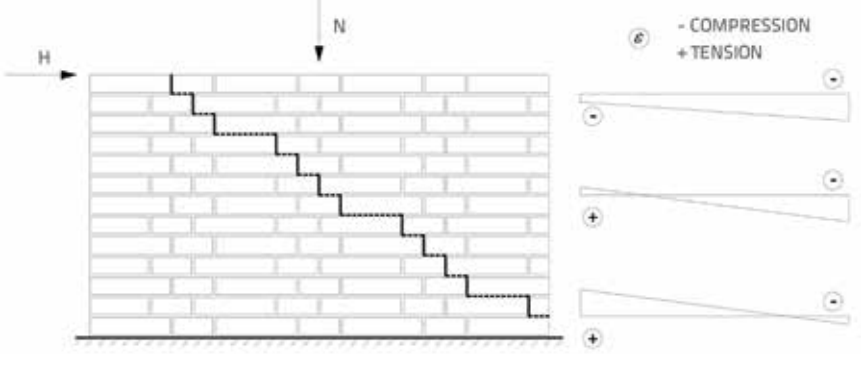

Figure 9. Change in length of the area in compression along the height of the wall

Clamping coefficient is the ratio of the height of the wall element to an average length of the overlap of two wall elements. In other words, ϕ represents an average slope of the failure surface (the tangent of the angle at which the stepped failure propagates). The load-bearing capacity limit at stepped failure is:

$$V_{d,lim} = \frac{1}{\gamma_{Rd}} \cdot L \cdot t_w \cdot \frac{f_{bt}}{2,3 \cdot b} \cdot \sqrt{1+\frac{\sigma_0}{f_{bt}}} \qquad (7)$$

where:

f_{bt} - tensile strength of the wall element.

If there are no more accurate data, the tensile strength of the wall element can be assumed as amounting to 10% of compressive strength of the wall element. It is important to note that the entire length of the wall is considered in Eq. (6), rather than only the compressed part as in Eq. (2), which is logical because the failure occurs along a series of joints. However, the clamping coefficient and the geometry factor are important changes with respect to Eq. (2).

4. Shear strengthening of masonry with non-metallic reinforcement

Shear strengthening of masonry can be ensured by adding TRM mesh or by gluing FRP strips to the wall. Several guidelines and standards are used for calculating the load-bearing capacity of strengthened structures. According to [42], the following proposals can currently be used to estimate the load-bearing capacity of FRP-strengthened structures: *fib* bulletin 14 [19], CNR-DT 200/2013 [43] and ACI 440.2R-02 [44], while CNR-DT 215/2018 [45] and ACI 549.4R-13 can be used for assessing load-bearing capacity of structures strengthened with TRM [46]. Although the standards [44] and guidelines [19] are intended for reinforced concrete structures, the methods for calculating strengthening will be shown with modifications suitable for masonry structures. Guideline [43] is intended for strengthening masonry with FRP, and so the following considerations will be based on that guideline.

4.1. Bases for analysis

The shear capacity of the strengthened wall (for both FRP and TRM) can be determined as:

$$V_{Rd} = V_{z,Rd} + V_{t,f} \qquad (8)$$

where:

$V_{z,Rd}$ - shear capacity of the unstrengthened wall

$V_{t,f}$ - strengthening shear capacity.

Eq. (8) is suitable for undamaged walls, while it can be considered that the load-bearing capacity of an unstrengthened wall is $V_{z,Rd}$ = 0 for significantly damaged walls. In both cases, crushing failure as well as other failure modes must be avoided (overturning,

out of plane failure, etc.). In both cases of strengthening, anchoring is a bigger problem than fibre failure. When anchoring, the conditions of strengthening exposure are important. The allowable design strain ε_{fd} can be determined using the Eq. (9):

$$\varepsilon_{fd} = \eta \cdot \frac{\varepsilon_{fk}}{\gamma_m} \quad (9)$$

where:
η - factor dependant on wall exposure conditions
ε_{fk} - characteristic strain at failure
γ_m - partial safety factor.

Exposure factor values for FRP are given in Table 1.

Table 1. exposure factor (from [43])

Exposure conditions	Fibre material	η
Internal	glass aramid carbon	0.75 0.85 0.95
External	glass aramid carbon	0.65 0.75 0.85
Aggressive	glass aramid carbon	0.50 0.70 0.85

Exposure factor values for TRM can be expressed in a simplified manner, independent of the fibre material. The values are given in Table 2.

Table 2. exposure factor (from [45])

Exposure conditions	η
Internal	0.9
External	0.8
Aggressive	0.7

The partial safety factor according to [43] is 1.2 for FRP for the ultimate limit state (ULS), while it is 1.5 for TRM according to [45]. The values refer to the loss of adhesion to the material for which a certificate about its characteristics is available. Characteristic strain at failure is less than the value of strain at loss of adhesion $\varepsilon_{lim,conv}$ and the value at tensile failure of fibres $\varepsilon_{u,f}$. The value of $\varepsilon_{u,f}$ is given by the manufacturer for both strengthening methods, while the determination of $\varepsilon_{lim,conv}$ is different for FRP and TRM as will be explained later on in the paper.
Based on the allowable design strain, allowable stress can be determined as:

$$f_{fd} = \varepsilon_{fd} \cdot E_f \quad (10)$$

where:
E_f - modulus of elasticity of fibre material (provided by the manufacturer).

4.2. Strengthening of masonry with FRP

FRP strengthening is achieved by gluing strips. Depending on the configuration of strips, the load-bearing capacity increase may be either higher or lower. Various recommendations for the calculation of strengthening are currently available. A detailed analysis of a number of such recommendations is given in [47], together with appropriate experimental laboratory data and field tests data. An overview of various recommendations is given below.

4.2.1. Strengthening design according to CNR-DT 200/2013

As the basic form of failure is the loss of adhesion of FRP and masonry, the allowable stress will depend on the length of the bonded area. The maximum length at which anchoring is achieved (further increase does not increase allowable stresses) can be determined according to [43] by the Eq. (11):

$$l_e = \max\left(\frac{1}{\gamma_{Rd} \cdot \tau_{bd}} \cdot \sqrt{\frac{\pi^2 \cdot E_f \cdot t_f \cdot \Gamma_{Fd}}{2}} \; ; 150 \text{ mm} \right) \quad (11)$$

where:
γ_{Rd} - safety factor (depending on the material)
τ_{bd} - adhesion strength
t_f - FRP strip thickness
Γ_{Fd} - design value of specific fracture energy.

According to [43], the safety factor of 1.5 can be assumed for tuff and perforated stone, while the safety factor of 1.25 can be assumed for limestone and calcarenite. It should be noted that the safety factor is not defined if a masonry wall is made of clay wall elements; however, the calculation will be on the side of safety if the factor of 1.25 is adopted. The adhesion strength can be determined by the Eq. (12):

$$\tau_{bd} = \frac{2 \cdot \Gamma_{Fd}}{s_u} \quad (12)$$

where:
s_u - slippage at failure.

According to [43] slippage at failure of 0.4 mm can be assumed for tuff stones and perforated bricks, while 0.3 mm is assumed for limestone and calcarenite. The value s_u for clay wall elements is also not defined here. The assumption that s_u = 0.3 mm can be adopted for clay wall elements is on the side of safety. The design value for specific fracture energy is:

$$\Gamma_{Fd} = \frac{k_b \cdot k_G}{FC} \cdot \sqrt{f_{bm} \cdot f_{btm}} \quad (13)$$

where:
k_b - geometry correction factor
k_G - correction factor dependent on the type of masonry
FC - confidence factor
f_{bm} - mean value of compressive strength of the wall element
f_{btm} - mean value of tensile strength of the wall element.

Correction factor depending on the type of masonry is 0.031 mm for perforated brick, 0.048 mm for tuff, and 0.012 mm for limestone and calcarenite. For prefabricated systems (e.g. FRP strips), the k_G should be reduced to 40 % of its value. The confidence factor is not explained in [43], but is described in NTC2018 [48]; *FC* can assume values of 1.0, 1.2 or 1.35, where the lowest value corresponds to the most detailed examination and 1.35 to the least detailed one. According to the new proposal of EN 1998-3 [34], three levels of confidence are also given, but the amounts of confidence factors depend on the masonry failure mode. A low level of confidence is when no tests have been performed (only a detailed visual inspection), a medium level is attributed if non-destructive tests have been performed and a high level of confidence is given if non-destructive tests and material characteristic tests have been performed (partially destructive or destructive tests). The mean tensile strength value of the wall element according to [43] can be estimated as $0.1 \cdot f_{bm}$. In the absence of experimental data, the geometry correction factor can be determined as follows:

$$k_b = \sqrt{\frac{3 \cdot l_f / b}{1 + l_f / b}} \tag{14}$$

where:

l_f - width of one FRP strip

b - width of the area of the strengthened element under the influence of the FRP strip.

In the case of regular elements, the width b can be determined as the width of the part of the wall on which the strip rests directly. Figure 10 shows the way in which the width b can be determined for horizontally and vertically glued strips.

In case of failure in the outer layer of the masonry, the allowable stress can be determined as:

$$f_{fd} = \frac{1}{\gamma_{f,d}} \cdot \sqrt{\frac{2 \cdot E_f \cdot \Gamma_{Fd}}{t_f}} \tag{15}$$

where:

$\gamma_{f,d}$ - safety factor that can be taken for loss of adhesion 1.2 according to [43].

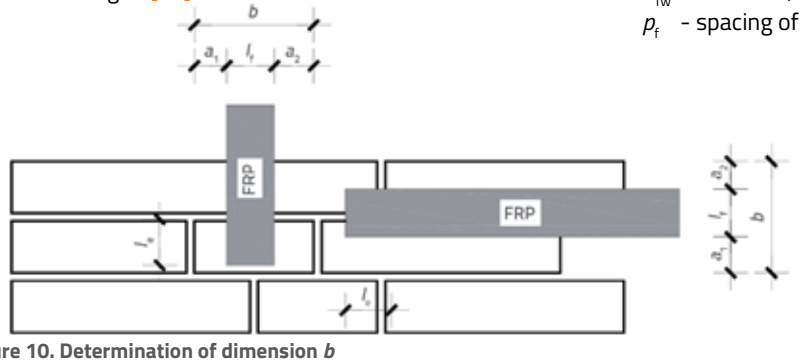

Figure 10. Determination of dimension *b*

Table 3. Allowed stress reduction coefficient for different ratios l_b / l_e

l_b / l_e	0.9	0.8	0.7	0.6	0.5	0.4	0.3	0.2	0.1
k	0.99	0.96	0.91	0.84	0.75	0.64	0.51	0.36	0.19

The maximum strain at failure can be determined by Eq. (10). If the length of the joint parallel to strip layout is less than the optimal bond length determined according to Eq. (11), the allowable stress determined by Eq. (15) should be reduced to 85 % of the value. The bond length should be determined experimentally in case anchors are used or FRP is bent around the wall. However, this length should be shorter than that obtained by Eq. (11) so that it can be used in these cases as well.

In case a shorter bond length is achieved, it is necessary to multiply the stress obtained by Eq. (15) by the coefficient:

$$k = \frac{l_b}{l_e} \cdot \left(2 - \frac{l_b}{l_e}\right) \tag{16}$$

where:

l_b - achieved bond length.

Allowable stress reduction factor values for various l_b / l_e ratios are given in Table 3.

If a part of a wall element can break off, a maximum of 80 % of the length of such element may be taken in the bond length. However, it is not suggested in [43] in which case a part of the brick actually breaks off. As shown in Table 3, if the bond length does not increase due to potential detachment of a wall element part, this condition leads to small reduction in allowable stress (only 4 % reduction for l_b / l_e = 0.8). Shear capacity of the masonry used in Eq. (8) is the sliding capacity determined by Eq. (2). Shear capacity of the FRP strengthening depends on the arrangement of FRP strips. In case the strips are placed parallel to the direction of shear force (horizontally in the case of walls) then shear capacity can be determined using the following Eq. (17):

$$V_{t,f} = \frac{1}{\gamma_{Rd}} \cdot \frac{0,6 \cdot d_f \cdot 2 \cdot A_{fw} \cdot f_{fd}}{p_f} \tag{17}$$

where:

γ_{Rd} - partial safety factor, which amounts to 1.2 according to [43]

d_f - distance from the strengthening fibre most stressed in tension and the masonry fibre most stressed in compression

A_{fw} - FRP area; $A_{fw} = l_f \cdot t_f$

p_f - spacing of adjacent FRP strips.

Figure 11 shows an example of strengthening with horizontal strips (and with vertical strips at wall extremities).

The maximum allowable strip spacing is not recommended in the standard. Obviously, it is necessary to have at least one strip per possible diagonal crack. Assuming a crack propagation at an angle of 45°, this would mean:

$$p_{f,max} = \min (0,5 \cdot h;\ 0,5 \cdot l_w) \tag{18}$$

However, Eq. (18) is not given in the

standard, but is rather assumed by the authors. A similar recommendation is given in [44] for strengthening RC elements where the maximum clear distance between two strips is $d_f / 4$. Eq. (18) should be modified for masonry depending on the morphology, masonry type, and element thickness. The authors are not familiar with the Eq. that takes into account characteristics of masonry. Although this condition is probably met in practical applications, it is important to ensure that a possible crack is retained by at least one strip.

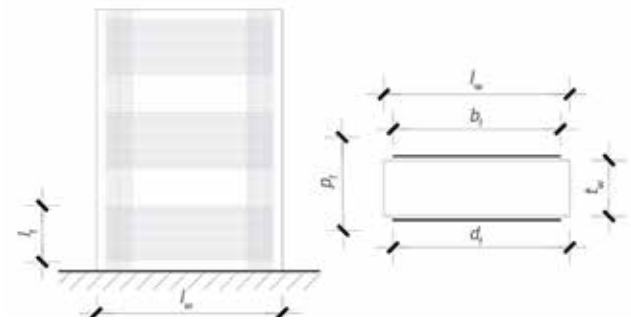

Figure 11. Schematic of horizontal strengthening with labels

For a different strengthening arrangement, a suitable mechanism should be adopted for the determination of shear capacity. For example, if a wall is strengthened as in Figure 12a), i.e. by two diagonal strips and two vertical ones, then a mechanism as shown in Figure 12b) can be formed. The influence of FRP in compression should be neglected. Based on the mechanism shown in Figure 12b), it is then easy to determine forces in each bar of the replacement truss. Thereafter, on the basis of the known widths and thicknesses of the individual strips, the load-bearing capacity of the vertical and diagonal strips can be determined by multiplying Eq. (15) by the cross-sectional area of the strip. Based on this, it is possible to determine at which level of horizontal force the failure occurs, and which strip will be the first to fail. The masonry contributes to the load-bearing capacity at a length equal to the length of the horizontal bar of the truss. In Figure 12b), dashed lines represent the elements in which compression occurs, while solid lines represent the elements in which tension occurs. Of course, during an earthquake, the force acts in both directions, and so strengthening must be placed symmetrically.

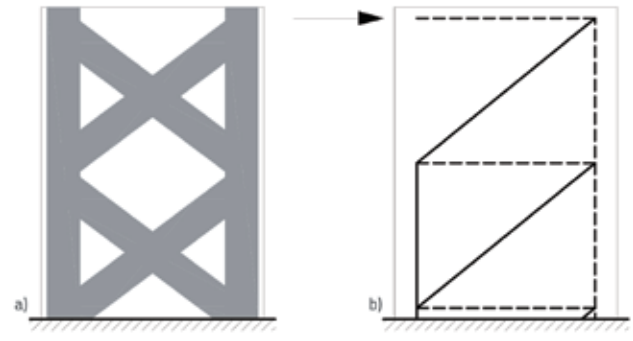

Figure 12. An example of masonry wall strengthening a) layout of strips; b) static scheme

In addition to tensile failure check, it is necessary to check that there is no compression failure of the wall. According to [43], the compression failure occurs by exceeding the force:

$$V_{Rd,max} = 0,3 \cdot f_{d,h} \cdot t_w \cdot d_f \tag{19}$$

where:
$f_{d,h}$ - design horizontal compressive strength of masonry.

The horizontal compressive strength of masonry is significantly lower than that in vertical direction [43], it can be assumed that $f_{d,h} = 0,5 \cdot f_d$.

4.2.2. Strengthening design according to ACI 440.2R-02 [44]

Shear capacity of FRP strengthening can be determined using the Eq.:

$$V_{t,f} = \phi_v \cdot \psi \cdot \frac{2 \cdot n \cdot t_f \cdot l_f \cdot d_f}{p_f} \cdot \varepsilon_{fd} \cdot E_f \cdot (\sin\alpha + \cos\alpha) \tag{20}$$

where:
ϕ_v - safety factor for shear, equal to 0.75
ψ - additional safety factor for FRP slippage, equal to 0.85
$2 \cdot n$ - total number of FRP mesh layers.

The calculation of the load-bearing capacity of the wall itself is different according to the ACI set of standards; however, neither this part of the load-bearing capacity nor the crushing will be elaborated here in greater detail. Design strain at failure depends on the arrangement of strips, on their bond length, and on the material to which FRP is attached, and can be determined as follows:

$$\varepsilon_{fd} = \kappa \cdot \varepsilon_{u,f} \leq 0,004 \tag{21}$$

where:
κ - strain reduction factor due to loss of adhesion.

Reduction factor can be determined using the Eq.:

$$\kappa = \left(\frac{f_{cm}}{27}\right)^{2/3} \cdot \frac{d_f - 2 \cdot L_e}{d_f} \cdot \frac{L_e}{11900 \cdot \varepsilon_{u,f}} \tag{22}$$

where:
L_e - active bond length.

Active bond length can be determined by the Eq.:

$$L_e = \frac{23300}{(n \cdot t_f \cdot E_f)^{0,58}} \tag{23}$$

4.2.3. Strengthening design according to fib bulletin 14 [19]

Although this guideline is intended for the calculation of strengthening of reinforced concrete structures, the calculation procedure will be presented with some adjustments for masonry. The load-bearing capacity of the FRP can be determined as:

$$V_{t,f} = 0,9 \cdot \varepsilon_{fd} \cdot E_f \cdot \rho_f \cdot t_w \cdot d_f \cdot (\sin\alpha + \cos\alpha) \quad (24)$$

where:

ρ_f - strengthening coefficient

α - angle between the FRP axis and wall axis.

The strengthening coefficient is $2 \cdot t_f \cdot \sin\alpha / t_w$ in the case of continuous gluing, or $(2 \cdot t_f / t_w) \cdot (l_f / p_f)$ in the case of gluing in strips. The design strain at failure can be determined by the Eq. (25):

$$\varepsilon_{fd} = 0,8 \cdot \min\left[0,65 \cdot \left(\frac{f_m^{2/3}}{E_f \cdot \rho_f}\right)^{0,56} \cdot 10^{-3} \; ; \; 0,17 \cdot \left(\frac{f_{cm}^{2/3}}{E_f \cdot \rho_f}\right)^{0,3} \cdot \varepsilon_{u,f}\right] \quad (25)$$

where:

f_m - compressive strength of the material (masonry).

The first Eq. in parentheses corresponds to the separation of the FRP, and the second to tensile failure. Also, this Eq. is defined for carbon fibres, and so its applicability is questionable.

It is also noted in the standard that a strain limit of 0.006 may be introduced to provide a shear transfer mechanism by mechanical clamping of the aggregate but, if it is not of crucial significance, such a limit is not necessary. In addition, this limitation does not seem necessary as the influence of mechanical clamping is not taken into account in the calculation of masonry, neither in the sliding mechanism nor in the diagonal tensile mechanism. It is important to note that a similar limitation exists in the norm [44], probably for the same reason. Also, as mentioned earlier, this standard also considers contribution of an unstrengthened element, and it is also necessary to avoid crushing of masonry.

4.3. Strengthening of masonry with TRM

4.3.1. Strengthening design according to CNR-DT 215/2018 [45]

The shear capacity of a strengthened wall can be determined using Eq. (8). It can be seen that the diagonal tensile capacity (straight failure) of an unstrengthened wall is taken into account in the final load-bearing capacity, which is in line with previous considerations. The shear capacity of masonry is the capacity to diagonal failure. Smaller value from $V_{t1,Rd}$ and $V_{t2,Rd}$ should be taken into account. The shear capacity of TRM strengthening is given in [45] by the Eq. (26):

$$V_{t,f} = \frac{1}{\gamma_{Rd}} \cdot n_f \cdot t_{Vf} \cdot l_f \cdot \alpha_t \cdot \varepsilon_{fd} \cdot E_f \quad (26)$$

where:

γ_{Rd} - partial safety factor, which amounts to 2.0 according to [45]

n_f - total number of strengthening layers (on both sides of the wall)

t_{Vf} - equivalent thickness of one strengthening layer in the shear direction

l_f - effective strengthening height

α_t - tensile strength reduction factor, which amounts to 0.8 according to [45]

ε_{fd} - allowable design strain of TRM

E_f - modulus of elasticity of TRM.

Eq. (26) is actually the area of all meshes ($n_f \cdot t_{Vf} \cdot l_f$) multiplied by strength ($\alpha_t \cdot \varepsilon_{fd} \cdot E_f$).

According to [45], if the strengthening is placed on one face of the wall, it is necessary to reduce $V_{Rd,f}$ by at least 30 % and anchors are mandatory. In other words, if the strengthening with two meshes is, for instance, 100 kN, the strengthening with one mesh is 50 · 0,7 = 35 kN. In the case of strengthening on one side of the wall, anchors should enter the last layer of the wall (the farthest layer from the strengthened face). In the case meshes are laid on both sides anchors are not necessary according to [45] except in the case of poor connection of masonry layers. The distance between anchors can be between $3 \cdot t_w$ and 160 cm in the case of wall thickness $t_w < 40$ cm. The distance between anchors can be between $2 \cdot t_w$ and 200 cm in the case wall thickness, t_w, is more than 40 cm. At the connection with transverse walls, an anchor should enter the transverse wall by at least $3 \cdot t_w$. However, according to the tests carried out in [49], it has been shown that such a large anchor spacing can lead to a local buckling of the strengthening, which is why the spacing approximately equal to the wall thickness is proposed. Large spacing of anchors enables the predicted increase in load-bearing capacity, but not a significant increase in ductility. However, as an increase in the ductility of the strengthened structure is not assumed in [45], the anchor spacing is acceptable. The number of anchors also affects the speed of construction and, currently, the number of tests is not large enough to reliably determine the impact of strengthening on the ductility of the structure.

The effective strengthening height is the height that contributes to shear capacity. Figure 13 shows a three-storey wall strengthened with TRM meshes. Assuming that the crack propagation angle is 45° as in [45], then the height that "holds" one crack is equal to the vertical projection of the length of that crack. If the wall is strengthened from top to bottom with TRM meshes and the floor height $h_s > l_w$, then $l_f = l_w$ and otherwise $l_f = h_s$, where h_s is the floor height and l_w is the wall length. Different conditions may be relevant for individual floors as can be seen in Figure 13.

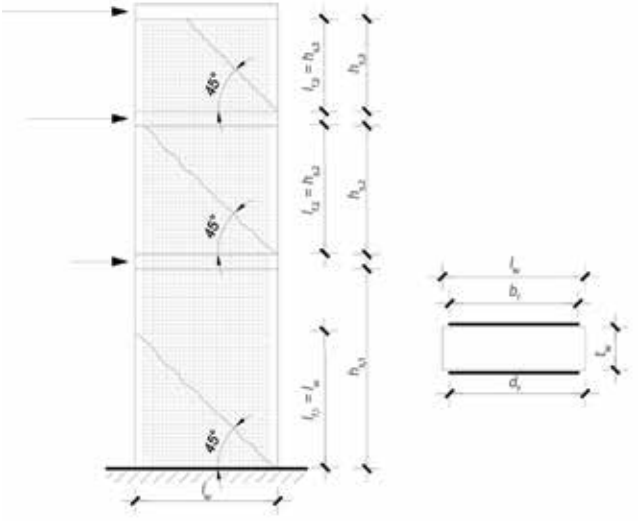

Figure 13. Masonry wall strengthened with TRM and diagonal cracks

Wall exposure factor values are given in Table 2.

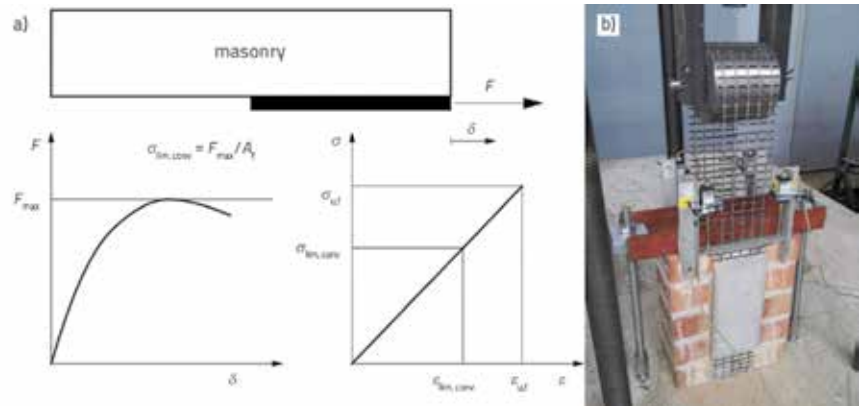

Figure 14. a) Schematic representation of adhesion test [45] b) sample adhesion testing [49]

Characteristic strain at failure is defined by the slippage of TRM mesh and, as it depends on the material of the mesh, matrix, and masonry, it has to be determined based on testing. According to [50], the manufacturer should provide the values $\varepsilon_{lim,conv}$ or $\sigma_{lim,conv}$ ($\sigma_{lim,conv} = E_f \cdot \varepsilon_{lim,conv}$) based on the adhesion test of masonry samples strengthened with TRM. Figure 14a schematically shows the method of determining adhesion according to [45], while the sample during testing is shown in Figure 14b [49].

It can be seen in Figure 14.a that the stress $\sigma_{lim,conv}$ is generally lower than the tensile strength at textile failure. The influence of multiple layers of meshes was examined in [25], where it was shown that the efficiency decreases for a larger number of layers. Overlapping of multiple layers causes reduction in the distance between the TRM fibres, leading to poorer connection between the mesh and mortar. For a larger number of layers, the stress is significantly lower than the tensile strength of the mesh. Also, the failure is less ductile due to poor adhesion caused by dense mesh.

As the test determined the adhesion at anchorage point, the allowed deformation can be increased by 50 % in the area far enough from the anchorage point according to [45] because the separation of the mesh can also occur at places away from the anchorage (but at higher deformation). Of course, if the deformation during separation is greater than that at which the tensile failure of the fibres $\varepsilon_{u,f}$ occurs, then $\varepsilon_{u,f}$ is adopted as allowable deformation. Figure 15a shows a sketch of a wall without openings, with obliquely hatched area where minor deformation is allowed (it is not defined in [45] which is the exact area where minor deformation is allowed, but the author's assumption is that it is an area < 30 cm from all ends of the mesh, because it is the bond length according to [45]).

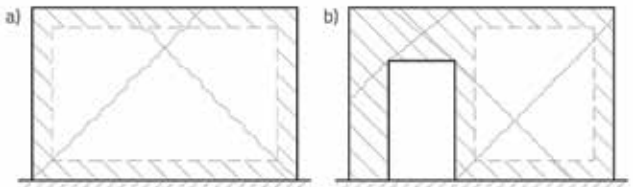

Figure 15. Layout of areas with allowable deformations: a) example 1; b) example 2

It can be seen in Figure 15a that, for this specific case, a large part of the mesh cutting the crack can be activated to a greater deformation (as the shaded area is small). Figure 15b shows a wall with an opening near the edge. It can be seen that for this specific case a higher allowable deformation is acceptable only for the part of the wall to the right of the opening, while a lower value is relevant for the part to the left of the opening and for the lintel. Accordingly, the allowable deformation must be determined based on the wall geometry and the expected location of the crack.

In addition to the above, in the case the anchoring of vertical strengthening is provided for, it is necessary to check crushing of masonry in the compression area. According to [45], the following Eq. can be used:

$$V_{Rd,max} = 0,25 \cdot f_d \cdot t_w \cdot d_f \quad (27)$$

where:
- f_d - design compressive strength of masonry
- t_w - wall thickness
- d_f - distance from the most stressed strengthening fibre in tension and the most stressed masonry fibre in compression.

The required bond length depends on the materials of the masonry, matrix and strengthening, and in the case it is not known, the value of 30 cm can be assumed according to [45].

4.3.2. Strengthening design according to ACI 549.4R-13 [46]

According to American standard ACI 549.4R-13 [46], the effect of strengthening can be determined by the Eq.:

$$V_f = 2 \cdot n \cdot A_f \cdot L \cdot f_{fv} \quad (28)$$

where:
- $2 \cdot n$ - total number of TRM mesh layers
- A_f - surface of one TRM layer per one meter of wall height
- L - wall length
- f_{fv} - design tensile strength of TRM.

The final load-bearing capacity of a strengthened wall can be determined by the Eq.:

$$V_{Rd} = \phi_v \cdot (V_f + V_m) \quad (29)$$

where:
- ϕ_v - safety factor for shear, which is 0.75
- V_m - shear bearing capacity of unstrengthened wall.

The design tensile strength of TRM can be determined as $E_f \cdot \varepsilon_{fv}$, , where ε_{fv} is limited to 0.004. The reason for the limitation

Table 4. Assumed masonry characteristics in the calculation example

f_{v0} [MPa]	σ_d [MPa]	σ_0 [MPa]	*KL*	L_c [cm]	t_w [cm]	h [cm]	L [cm]	f_t [MPa]	ϕ	f_b [MPa]	f_{bt} [MPa]
0.16	1.33	0.5	2	75	30	300	200	0.11	1.0	15	1.5

is that the load-bearing component of the masonry cannot be counted on for larger strains. A comparison of Eq.s (26) and (28) shows that they are very similar, but some differences do exist. Symmetrical placement of meshes on both sides of the wall is assumed in [46] (hence 2·*n*). The mesh surface is reduced to one meter in height, which is multiplied by the length of the wall. Thus l_f from Eq. (26) is reduced to *L*. This is fine for slender walls, but for long and low walls it could lead to an unrealistically high load-bearing capacity. In this standard, it is noted that the influence of eccentricity should be considered in the case of eccentric strengthening.

5. Calculation example

The following is an example of calculation of the load-bearing capacity of an undamaged wall strengthened with FRP and TRM. The materials of the wall element are solid brick and lime mortar. The dimensions of the brick elements are *h*/*w*/*l* = 6,5/15/30 cm and the horizontal bed-joints are on an average 1.0 cm thick. In this example, the load-bearing capacity of an unstrengthened masonry is determined in the same way, regardless of which guideline is used for the calculation of strengthening. Thus, it is easier to compare the contribution of strengthening according to a particular standard. The design compressive force is N_{Ed} = 300 kN. The load eccentricity is *e* = 75 cm, and so the bending moment on the wall is M_{Ed} = 225 kNm. Assuming that the wall is statically clamped on both sides, the shear force is V_{Ed} = 150 kN.

Masonry wall characteristics should be determined for each structure by visual inspection and testing. Here, these characteristics are assumed, and their values are given in Table 4. The value of *KL* represents the level of knowledge, with 2 being an intermediate level of knowledge.

According to Eq. (1), the shear strength is f_v = 0.16 + 0.5 · 1.33 = 0,83 MPa but it must not exceed 0,065 · 15 = 0.98 Mpa. According to Eq. (2), the load-bearing capacity of a wall for sliding is $V_{p,Rd}$ = 1 / 1.5 · 0. 83 · 750 · 300 = 124500 N = 124,5 kN.

The ratio *b* = *h*/*L* is 1.5 and, according to Eq. (4), the allowable shear stress is τ = 0.11 / 1.5 · √(1 + 0.5 / 0.11) = 0.17 MPa. According to Eq. (5), the load-bearing capacity of the wall for the diagonal straight failure is $V_{t1,Rd}$ = 1 / 1.55 · 2000 · 300 · 0.11 / 1.5 · √(1 + 0.5 / 0.11) = 66848 N = 66.85 kN.

According to Eq. (6), the load-bearing capacity of the wall for the diagonal stepped failure is $V_{t2,Rd}$ = 1 / 1.55 · 2000 · 300 / 1.5 · [0.16 / (1 + 0.6 · 1.0) + 0.6 · 0.5 / (1 + 0.6 · 1.0)] = 74194 N = 74.19 kN. The limit value according to Eq. (7) is $V_{d,lim}$ = 1 / 1.55 · 2000 · 300 · 1.5 / (2.3 · 1.5) · √(1 + 0.5 / 1.5) = 194340 N = 194.34 kN.

The load-bearing capacity of an unstrengthened wall for sliding failure is $V_{p,Rd}$ = 124.5 kN and the load-bearing capacity for diagonal failure is $V_{t,Rd}$ = 66.85 kN. It can be seen that there is a diagonal failure mode of the unstrengthened wall because V_{Ed} = 150 kN > V_{Rd} = 66.85 kN. The wall needs to be strengthened.

5.1. Strengthening of masonry with FRP

The following is an example of strengthening of an undamaged wall with prefabricated horizontal and vertical carbon FRP strips (lamellas) on both sides of the wall, as shown in Figure 11. The wall under study has no openings. The characteristics of the material should be defined by the manufacturer based on appropriate tests. Here, these characteristics are assumed, and their values are shown in Table 5.

Table 5. Assumed FRP characteristics in the calculation example

E_f [MPa]	t_f [cm]	l_f [cm]	d_f [cm]	$\varepsilon_{u,f}$ [%]
170000	0.1	10	195	1.6

The axial distance of the lamellas p_f is determined to ensure sufficient load-bearing capacity.

It is also assumed that the mean vertical compressive strength of the masonry is 3.4 MPa. According to the guideline [43], it can be assumed that the horizontal compressive strength of the wall is $f_{d,h}$ = 0.5 · 3.4 = 1.7 MPa. According to Eq. (19), the maximum allowable force (which causes masonry to crush) is $V_{Rd,max}$ = 0.3 · 0.17 · 30 ·195 = 298.35 kN.

5.1.1. Strengthening design according to CNR-DT 200/2013 [43]

A correction factor of k_G = 0.031 mm, corresponding to perforated brick, is assumed. As solid brick was used in the example, the fracture energy should be slightly higher, but the guideline [43] does not give the values of the correction factor. Also, this value is reduced to 40 % because prefabricated FRP elements (lamellas) were used, i.e. k_G = 0.031 · 0.4 = 0.012 mm. It is assumed that only a detailed visual inspection was performed, and so the confidence factor is *FC* = 1.35. Horizontal lamellas used in this example can be glued so that they are in contact with two or three bricks. More bricks mean lower fracture energy and lower allowable stress. For safety reasons, the lamellas are assumed to be in contact with three bricks along the height. In accordance with Figure 10, b = 3 · 6.5 + 2 · 1.0 = 21.5 cm and the correction factor according to Eq. (14) is k_b = √[(3 · 10 / 21.5) / (1 + 10 / 21.5)] = 0.98. According to Eq. (13), the fracture energy is Γ_{Fk} = 0.012 · 0.98 / 1.35 · √(15 · 1.5) = 0.041 N / mm.

According to Eq. (15), the allowable stress is f_{fd} = 1 / 1.2 · √(2 · 170000 · 0.041 / 1.0) = 98.39 MPa.

It is assumed that slippage at failure is 0.3 mm, which should be

conservative. The allowable shear stress according to Eq. (12) is τ_{bd} = 2 · 0.041 / 0.3 = 0.27 MPa. The bond length according to Eq. (11) is l_e = max[1 / (1.25 · 0.27) · √(π² · 170000 · 1.0 · 0.041 / 2) ; 150 mm] = max[550 ; 150] = 550 mm. As the required bond length is shorter than the length of the compression area in critical section (the section in which the length of the compression area is the shortest), it is considered that the full bond length is provided for all strips.

The load-bearing capacity of the unstrengthened wall is 124.5 kN and should be 150 kN. This means that the following should be achieved by strengthening: $V_{t,f}$ = 150 – 124.5 = 25.5 kN.

According to Eq. (17) the shear capacity of the FRP strengthening is $V_{t,f}$ = 0.6 · 1950 · 2 · 100 · 1.0 · 98.39 / (1.2 · p_f) ≥ 25500 N. It follows that the distance p_f ≤ 0.6 · 1950 · 2 · 100 · 1.0 · 98.39 / (1.2 · 25500) = 752 mm. The distance p_f = 75 cm is selected.

The load-bearing capacity of the strengthening with the selected spacing is $V_{t,f}$ = 0.6 · 1950 · 2 · 100 · 1.0 · 98.39 / (1.2 · 750) = 25581 N = 25.56 kN.

The final load-bearing capacity of the strengthened wall is $V_{Rd,CNR}$ = 124.5 + 25.56 = 150.06 kN. In this case, an increase in the load-bearing capacity due to strengthening is 21 %.

5.1.2. Strengthening design according to ACI 440.2R-02 [44]

The bond length of one strip according to Eq. (23) is l_e = 23300 / (2 · 1.0 · 17000)^{0,58} = 54.84 cm. The reduction coefficient according to Eq. (22) is κ = (0.5 / 27)$^{2/3}$ · (195 – 2 · 54.84) / 195 · 54.84 / (11900 · 0.016) = 0.00882. Design strain at failure according to Eq. (21) is ε_{fd} = 0.00882 · 0.016 = 0.000141 < 0.004.

If the same strip spacing is selected as in the example according to [43] the shear capacity of the FRP strengthening according to Eq. (20) is $V_{t,f}$ = 0.75 · 0.85 · 2 · 2 · 0.1 · 10 · 195 · 0.000141 · 17000 · (sin(90°) + cos(90°)) / 75 = 15.89 kN.

The final load-bearing capacity of the strengthened wall is $V_{Rd,ACI}$ = 124.5 + 15.89 = 140.39 kN. In this case, an increase in the load-bearing capacity due to strengthening is 13 %.

In order to ensure the required load-bearing capacity according to [44] it is necessary to provide a distance p_f ≤ 0.75 · 0.85 · 2 · 2 · 0.1 · 10 · 195 · 0.000141 · 17000 · (sin(90°) + cos(90°)) / 25.5 = 46.74 cm. If the distance p_f = 45.0 cm is chosen, the load-bearing capacity of the strengthening is $V_{t,f}$ = 26.2 kN, i.e. the total load-bearing capacity is $V_{Rd,ACI}$ = 124.5 + 26.2 = 150.7 kN. In this case, an increase in the load-bearing capacity due to strengthening is 21 %.

5.1.3. Strengthening design according to fib bulletin 14 [19]

The FRP strengthening coefficient is ρ_f = 2 · 1.0 / 30 · 10 / 75 = 0.0089. According to Eq. (25) the allowable strain is ε_{fd} = 0.8 · min[0.65 · (3.4$^{2/3}$ / (170000 · 0. 0089))$^{0.56}$ · 10^{-3} ; 0.17 · (3.4$^{2/3}$ / (170000 · 0. 0089))$^{0.3}$ · 0.016] = 0.8 · min[0.000017 ; 0.000386] = 0.8 · 0. 000017 = 0.0000136. According to Eq. (24) the shear capacity of the FRP strengthening is $V_{t,f}$ = 0.9 · 0.0000136 · 170000 · 0.0089 · 300 · 1950 · (sin(90°) + cos(90°)) = 10834 N = 10.83 kN.

The final load-bearing capacity of the strengthened wall is $V_{Rd,FIB}$ = 124.5 + 10.83 = 135.33 kN. In this case, an increase in the load-bearing capacity due to strengthening is 9 %.

The smallest possible axial distance of the lamellas is 10 cm and, for that distance, according to [19], the total load capacity is $V_{Rd,FIB}$ = 157.48 kN, which is greater than 150 kN.

5.1.4. Comparison of calculation results

If calculation results are compared according to individual guidelines, it is evident that the highest contribution of strengthening was obtained according to guideline CNR-DT 200/2013 [43] and the lowest according to fib bulletin 14 [19]. However, guidelines [19] and ACI 440.2R-02 [44] are primarily intended for calculating strengthening of concrete structures. Also, guideline [43] is the most detailed and calculation according to this guideline is somewhat more complicated. Therefore, it is expected that this guideline gives the largest increase in load-bearing capacity, while the remaining guidelines are more conservative.

5.2. Strengthening of masonry with TRM

The following is an example of strengthening of an undamaged wall with TRM placed along the entire height on both sides of the wall, as shown in Figure 13. Carbon meshes are used in the example and the wall is assumed to be external (environmental conditions are not aggressive). The observed wall has no openings. The characteristics of the material should be defined by the manufacturer based on appropriate tests. Here, the characteristics are assumed, and their values are shown in Table 6.

Table 6. Assumed TRM characteristics in the calculation example

E_f [MPa]	t_f [cm]	d_f [cm]	ε_{fk} [%]
170000	0.0048	195	0.65

The total number of meshes n_f will be determined in such a way to ensure sufficient load-bearing capacity.

The maximum allowable force (which causes masonry to crush) according to Eq. (27) is $V_{Rd,max}$ = 0.25 · 0.34 · 30 · 195 = 497.25 kN.

5.2.1. Strengthening design according to CNR-DT 215/2018 [45]

The exposure factor for carbon fibre is 0.95 for the inner layer and 0.85 for the outer layer. A mean value of 0.9 is taken into account. The allowable design strain ε_{fd} according to Eq. (9) is ε_d = 0.9 · 0.0065 / 1.5 = 0.0039. Since L < h, then l_f = L = 200 cm.

For one mesh on each face of the wall according to Eq. (26) the shear capacity of the TRM strengthening is $V_{t,f}$ = 1 / 2 · 2 · 0.048 · 2000 · 0.8 · 0.0039 · 170000 = 50918 N = 50.92 kN.

The final load-bearing capacity of the strengthened wall is

$V_{Rd,CNR}$ = 66.85 + 50.92 = 117.77 kN. In this case, an increase in the load-bearing capacity due to strengthening is 76 %.
For two layers of mesh on each face of the wall according to Eq. (26) the shear capacity of the TRM strengthening is $V_{t,f}$ = 1 / 2 · 4 · 0.048 · 2000 · 0.8 · 0.0039 · 170000 = 101837 N = 101.84 kN.
The final load-bearing capacity of the strengthened wall is $V_{Rd,CNR}$ = 66.85 + 101.84 = 168.69 kN. In this case, an increase in the load-bearing capacity due to strengthening is 152 %.
However, according to [25] the effect of two or more layers is significantly reduced, and so it is questionable whether a double increase in load-bearing capacity would be justified.
For this reason, it seems more appropriate to choose FRP strengthening in this example.

5.2.2. Strengthening design according to ACI 549.4R-13 [46]

As the allowed strain is greater than 0.4 %, the value ε_{fd} = 0.004 is taken into account. For one mesh on each face of the wall according to Eq. (28), the shear capacity of the TRM strengthening is $V_{t,f}$ = 2 · 1 · 0.048 · 2000 · 0.004 · 170000 = 130560 N = 130.56 kN.
The final load-bearing capacity of the strengthened wall is $V_{Rd,CNR}$ = 0.75 · (66.85 + 130.56) = 148.06 kN. In this case, an increase in the load-bearing capacity due to strengthening is 121 %. According to this standard, the shear load-bearing capacity is also not satisfied by placing one layer of TRM on each face of the wall, and so it is necessary to place two layers.

5.2.3. Comparison of calculation results

Comparison of calculation results shows that a higher contribution of strengthening is obtained by the ACI 549.4R-13 standard [46]. The main difference in calculations according to each guideline is the method for calculating allowable strain. In case it is significantly higher than 0.4 %, guideline CNR-DT 215/2018 [45] would give higher load-bearing capacity values than the standard [46]. Guideline [45] provides more partial safety factors, while the standard [46] provides a global factor that further reduces the unstrengthened load-bearing component of the wall. Therefore, guideline [45] seems more suitable for use in combination with the standard EN 1998-3 [34].

6. Conclusion

Unreinforced unconfined masonry is highly sensitive to lateral forces. The basic failure modes are caused by bending or, more often, by shear. There are three basic shear failure modes: sliding, exceeding diagonal tensile stresses, and stepped diagonal failure. Which one of these will prevail depends on the intensity of vertical pressure, typology of masonry, and quality of material. In order to increase shear capacity, masonry can be strengthened with metallic or non-metallic reinforcement. Both methods present some advantages, but also some disadvantages. Before strengthening, it is important to identify possible failure modes, and the strengthening schedule should be determined depending on the geometry of the masonry and local conditions of the building. Non-metallic reinforcement can be bonded to masonry with epoxy adhesive (FRP) or mortar (TRM). This paper presents current guidelines and regulations for determining the in-plane shear capacity of masonry buildings before and after their strengthening. For both types of strengthening (FRP and TRM), the loss of adhesion is the primary failure mode and the values of strain at failure should be given by the manufacturer based on testing. The Eq.s for the load-bearing capacity calculation depend on the strengthening arrangement and consist of the load-bearing component and strengthening component. The load-bearing component of masonry depends on the condition of masonry before strengthening, and should not be taken with full value for damaged masonry, but the standards do not provide accurate guidelines. Although anchors are required for unilateral TRM strengthening, there are no anchor spacing recommendations for other forms of strengthening. However, the recommended anchor spacing does not ensure stability of the strengthening, and so the guidelines do not provide instructions on any change in the ductility of the system. It is assumed that only the load-bearing capacity of elements is increased, and that the ductility and stiffness remain unchanged. The guidelines can be used to determine the load-bearing capacity of masonry strengthened with FRP or TRM in a relatively simple way, as shown by an example presented in the paper. Out of presented guidelines and standards, the most suitable for use in Croatia are the CNR guidelines (for both FRP and TRM) due to their level of detail, good compatibility with the EN 1998-3 standard, and similar typology of masonry in Croatia and Italy.

Acknowledgments

A part of this research was funded by the Croatian Science Foundation, the ARES project: Assessment and rehabilitation of existing structures – development of contemporary methods for masonry and timber structures (UIP-2019-04-3749). The authors are grateful for the support.

REFERENCES

[1] Simović, V.: Potresi na zagrebačkom području, Građevinar, 52 (2000) 11, pp. 637–645.

[2] Kuk, V., Prelogovi, E., Sovi, I., Kuk, K., Šariri, K.: Seizmološke i seizmotektonske značajke šireg zagrebačkog područja, Građevinar, 52 (2000) 11, pp. 647–653.

[3] Stepinac, M., Kišiček, T., Renić, T., Hafner, I., Bedon, C.: Methods for the assessment of critical properties in existing masonry structures under seismic loads-the ARES project, Applied Sciences (Switzerland), 10 (2020) 5.

[4] Atalić, J., Šavor Novak, M., Uroš, M.: Rizik od potresa za Hrvatsku: pregled istraživanja i postojećih procjena sa smjernicama za budućnost, Građevinar, 71 (2019) 10, pp. 923–947.

[5] Stepinac, M., Rajčić, V., Žarnić, R.: Timber-structural glass composite systems in earthquake environment, Gradjevinar 68 (2016) 3, pp. 211–219.

[6] Beeson, S., Kubin, J., Unav, A.I.: Potresna osjetljivost povijesnih zidanih konstrukcija nepravilne geometrije, Gradjevinar 67 (2015) 2, pp. 151–158.

[7] Sorić, Z.: Zidane konstrukcije, Zagreb, 2016.

[8] Tomaževič, M.: Protupotresna obnova postojećih zidanih građevina, Građevinar, 52 (2000) 11, pp. 683–693.

[9] Bhattacharya, S., Nayak, S., Dutta, S.C.: A critical review of retrofitting methods for unreinforced masonry structures, International Journal of Disaster Risk Reduction, 7 (2014), pp. 51–67.

[10] Sorić, Z., Kišiček, T., Galić, J.: "Deflections Of Concrete Beams Reinforced With FRP Bars", Materials and Structures (2010) 43:73-90, Springer Netherlands, DOI 10.1617/s11527-010-9600-1.

[11] Zoghi, M. (ur.): The International Handbook of FRP Composites in Civil Engineering, CRC Press, Boca Raton, 2013.

[12] Bakis, C.E., Bank, L.C., Brown, V.L., Cosenza, E., Davalos, J.F., Lesko, J.J., Machida, A., Rizkalla, S.H., Triantafillou, T.C.: Fiber-reinforced polymer composites for construction - State-of-the-art review, Journal of Composites for Construction, 6 (2002) 2, pp. 73–87.

[13] Sika Group, www.sika.com/en/construction/structural-strengthening/fiber-reinforced-polymer-fabrics.html, 25.05.2020.

[14] Calabrese, A.S., D'Antino, T., Poggi, C., Colombi, P., Fava, G., Pisani, M.A.: Application of Externally Bonded Inorganic-Matrix Composites to Existing Masonry Structures, Springer International Publishing, pp. 283-292, 2020.

[15] Benmokrane, B., Ali, A.H.: Durability and Long-Term Performance of Fiber-Reinforced Polymer as a New Civil Engineering Material, International Congress on Polymers in Concrete (ICPIC 2018), New Mexico, pp. 49-59, 2018.

[16] Yu, F., Li, Z., Yuan, F., Zhu, D., Kong, Z.: Mehanička svojstva spoja betonskog stupa ovijenog PVC-CFRP-om i AB grede pri osnom opterećenju, Građevinar, 72 (2020) 2, pp. 151–164.

[17] Carić, M., Kišiček, T.: Pojačanja nearmiranog zida tkaninom armiranim mortovima (TRM) na posmik, Simpozij doktorskog studija Građevinarstva 2017, Zagreb, pp. 49-59, 2017.

[18] Risan, H.K., Harba, I.S.I., Abdulridha, A.J.: Numerička analiza ab zida s otvorom ojačanim CFRP-om podvrgnutim ekscentričnim opterećenjima, Gradjevinar, 69 (2017) 7, pp. 573–580.

[19] fib bulletin 14 – Externally bonded FRP reinforcement for strengthening RC structures, fib: Lausanne, Switzerland, 2004.

[20] Sorić, Z., Kišiček, T.: BETONSKE KONSTRUKCIJE 3. Projektiranje betonskih konstrukcija prema europskim normama EN. Skripta Građevinskog fakulteta Sveučilišta u Zagrebu

[21] Caggegi, C., Lanoye, E., Djama, K., Bassil, A., Gabor, A.: Tensile behaviour of a basalt TRM strengthening system: Influence of mortar and reinforcing textile ratios, Composites Part B: Engineering, 130 (2017), pp. 90–102.

[22] Misseri, G., Rovero, L., Stipo, G., Barducci, S., Alecci, V., De Stefano, M.: Experimental and analytical investigations on sustainable and innovative strengthening systems for masonry arches, Composite Structures, 210 (2019), pp. 526–537.

[23] Kišiček, T., Carić, M.: Pojačanja armiranobetonskih konstrukcija pomoću tkaninom armiranih mortova, 1st International Conference on Construction Materials for Sustainable Future, Zagreb, pp. 754-761, 2017.

[24] Kouris, L.A.S., Triantafillou, T.C.: State-of-the-art on strengthening of masonry structures with textile reinforced mortar (TRM), Construction and Building Materials, 188 (2018), pp. 1221–1233.

[25] Ferrara, G., Caggegi, C., Gabor, A., Martinelli, E.: Experimental Study on the Adhesion of Basalt Textile Reinforced Mortars (TRM) to Clay Brick Masonry: The Influence of Textile Density, Fibers, 7 (2019) 12, pp. 103.

[26] De Felice, G., De Santis, S., Roscini, F.: Seismic Retrofitting of Cultural Heritage with Textile Reinforced Mortar, State of the Art, COST Action TU1207 Next Generation Design Guidelines for Composites in Construction, 2017.

[27] AC 434 – Acceptance Criteria for Masonry and Concrete Strengthening Using Fabric-Reinforced Cementitious Matrix (FRCM) Composite Systems, ICC-ES: California, USA, 2011.

[28] Al-Lami, K., D'Antino, T., Colombi, P.: Durability of fabric-reinforced cementitious matrix (FRCM) composites: A review, Applied Sciences (Switzerland), 10 (2020) 5.

[29] Gopinath, S., Madheswaran, C.K., Prabhakar, J., Thivya Devi, K.G., Lakshmi Anuhya, C.: Strengthening of Unreinforced Brick Masonry Panel Using Cast-in-Place and Precast Textile-Reinforced Concrete, Journal of Earthquake Engineering, (2020), pp. 1–19.

[30] Bisby, P.L., Stratford, T., Hart, C., Farren, S.: Fire performance of well-anchored TRM, FRCM and FRP flexural strengthening systems, Advanced Composites in Construction (ACIC 2013) - Conference Proceedings, Belfast, pp. 98–109, 2013.

[31] Türkmen, S., De Vries, B.T., Wijte, S.N.M., Vermeltfoort, A.T.: Türkmen, S., De Vries, B.T., Wijte, S.N.M., Vermeltfoort, A.T.: In-plane behaviour of clay brick masonry wallettes retrofitted with single-sided fabric-reinforced cementitious matrix and deep mounted carbon fibre strips, Bulletin of Earthquake Engineering, 18 (2020) 2, pp. 725-765.

[32] Lušo, R., Kišiček, T.: Sidrenje tkaninom armiranih mortova (TRM) i vlaknima armiranih polimera (FRP) pri pojačavanju armiranobetonskih i zidanih elemenata konstrukcija, Simpozij doktorskog studija Građevinarstva 2018, Zagreb, pp. 149-159, 2018.

[33] Ghiassi, B., Milani, G. (Ur.): Numerical modeling of masonry and historical structures from theory to application, Woodhead Publishing Limited, Duxford, UK, 2019.

[34] EN 1998-3-Eurocode 8: Design of Structures for Earthquake Resistance-Part 3: Assessment and Retrofitting of Buildings; CEN: Brussels, Belgium, 2004.

[35] HRN EN 1996-1-1:2012-Eurokod 6: Projektiranje zidanih konstrukcija-Dio 1-1: Opća pravila za zgrade. Pravila za armirane i nearmirane zidane konstrukcije (EN 1996-1-1:2005); CEN: Brussels, Belgija, 2005.

[36] Turnšek, V., Čačovič, F.: Some experimental results on the strength of brickmasonry walls, Proc 2nd Int Brick & Block Masonry Conference, Stoke-on-Trent; pp. 149–56, 1971.

[37] Tomaževič, M.: Shear resistance of masonry walls and Eurocode 6: Shear versus tensile strength of masonry, Materials and Structures/Materiaux et Constructions, 42 (2009) 7, pp. 889–907.

[38] Mann, W., Müller, H.: Failure of shear-stressed masonry - an enlarged theory, tests and application to shear walls, Proc. int. symposium on load-bearing brickwork, 1980, pp. 1–13.

[39] Magenes, G., Calvi, G.M.: In-Plane Seismic Response of Brick Masonry Walls, Earthquake Engineering and Structural Dynamics, 26 (1997), pp. 1091–1112.

[40] Lagomarsino, S., Penna, A., Galasco, A., Cattari, S.: TREMURI program: An equivalent frame model for the nonlinear seismic analysis of masonry buildings, Engineering Structures, 56 (2013), pp. 1787–1799.

[41] Kržan, M., Gostič, S., Cattari, S., Bosiljkov, V.: Acquiring reference parameters of masonry for the structural performance analysis of historical buildings, Bulletin of Earthquake Engineering, 13 (2015) 1, pp. 203–236.

[42] Bonati, A., Franco, A., Coppola, O., De Luca, G.: Strengthening of Masonry Structures: Current National and International Approaches for Qualification and Design, Key Engineering Materials, 817 (2019), pp. 501–506.

[43] CNR-DT 200 R1/2013 – Guide for the Design and Construction of Externally Bonded FRP Systems for strengthening Existing Structures, CNR.: Rome, Italy, 2013.

[44] ACI 440.2R-02 – Guide for the Design and Construction of Externally Bonded FRP Systems for Strengthening Concrete Structures, ACI: USA, 2002.

[45] CNR-DT 215/2018 – Guide for the Design and Construction of Externally Bonded Fibre Reinforced Inorganic Matrix Systems for strengthening Existing Structures, CNR.: Rome, Italy, 2018.

[46] ACI 549.4R-13 – Guide to Design and Construction of Externally Bonded Fabric Reinforced Cementitious Matrix (FRCM) Systems for Repair and Strengthening Concrete and Masonry Structures, ACI: MI, USA, 2013.

[47] Simonič, M.J., Bosiljkov, V., Žarnić, R.: Ispitivanje i analiza nosivosti na posmik zidova ojačanih s FRP-om, Građevinar, 66 (2014) 6, pp. 533–548.

[48] NTC08 – Supplemento ordinario alla "Gazzetta Ufficiale" n. 35 del 11 febbraio 2019 - Serie generale n. 7 C.S.LL.PP., Ministero delle infrasttruturee dei trasporti, Rome, Italy, 2019.

[49] Gams, M., Tomaževič, M., Berset, T.: Seismic strengthening of brick masonry by composite coatings: an experimental study, Bulletin of Earthquake Engineering, 15 (2017), pp. 4269–4298.

[50] Ascione, L., Carozzi, F.G., D'Antino, T., Poggi, C.: New Italian guidelines for design of externally bonded Fabric-Reinforced Cementitious Matrix (FRCM) systems for repair and strengthening of masonry and concrete structures, Procedia Structural Integrity, 11 (2018), pp. 202–209.